（ ※本報告書は英語で記述してください。ただし、産業利用課題として採択されている方は日本語で記述していただいても結構です。 ）

CROSS TOKAI **Experimental Report** J-PARC	承認日 Date of Approval 承認者 Approver 提出日 Date of Report
課題番号 Project No. 2015E0001 実験課題名 Title of experiment In-situ Neutron Diffraction Analysis of Deformation and Phase Transformation Behaviors of Advanced Structural Materials in Elements Strategy Initiative for Structural Materials (ESISM) 実験責任者名 Name of principal investigator Nobuhiro Tsuji 所属 Affiliation Kyoto University	装置責任者 Name of Instrument scientist BL:19: Kazuya Aizawa 装置名 Name of Instrument/(BL No.) BL19 実施日 Date of Experiment (1) 6/20-6/22, 2015 (2) 5/16, 17, 19, 20, 2016

試料、実験方法、利用の結果得られた主なデータ、考察、結論等を、記述して下さい。(適宜、図表添付のこと)
Please report your samples, experimental method and results, discussion and conclusions. Please add figures and tables for better explanation.

1. 試料 Name of sample(s) and chemical formula, or compositions including physical form.

(1) 6/20-6/22, 2015

Fe-2Mn-0.1C (wt. %), Fe-24Ni-6Al-0.4C (wt. %), Cu-40Zn (wt. %).

(2) 5/16, 17, 19, 20, 2016

Fe-2Mn-0.1C (wt. %), Fe-5Mn-2Si-0.1C (wt. %), Ti-6Al-4V (wt. %).

2. 実験方法及び結果（実験がうまくいかなかった場合、その理由を記述してください。）
Experimental method and results. If you failed to conduct experiment as planned, please describe reasons.

(1) 6/20-6/22, 2015

(1-1)

The cold-rolled Fe-24Ni-6Al-0.4C alloy exhibits extremely high strength but keeps reasonable elongation even in the as-rolled state. In order to clarify the origin of the superior mechanical properties, we conducted *in-situ* neutron diffraction experiment during tensile deformation of Fe-24Ni-6Al-0.4C alloys which were cold rolled with the reduction of 0 %, 50 %, and 81%.

As shown in the schematic illustration of Figure 1, a tensile test specimen was mounted at the standard tensile testing system at BL19 TAKUMI as that the tensile axis to be aligned 45° with respect

to the incident beam. The neutron diffraction patterns in the axial and transversal directions were measured simultaneously using two time-of-flight detector banks that have the scattering angles of ± 90°.

Figure 2 shows *in-situ* neutron diffraction profiles during tensile deformation of the 0 % cold-rolled specimen. The 0 % cold-rolled specimen before tensile deformation consisted of austenite (FCC) and intermetallic particles (BCC base structure). On the other hand, the peaks corresponding to martensite began to appear after tensile strain of about 30%.

Figure 3 summarizes changes in fraction of martensite with increasing of the tensile strain. We found that deformation-induced martensitic transformation occurred during tensile deformation even in the 50% and 81% cold-rolled specimens. In addition, the fractions of deformation induced martensite in the 50 % and 81 % cold-rolled specimens were much higher than that in the 0 % cold-rolled specimen. This results strongly suggest that transformation-induced plasticity happened by deformation-induced martensitic transformation is one of the main reason for the high strength and large ductility of the cold-rolled Fe-24Ni-6Al-0.4C alloy.

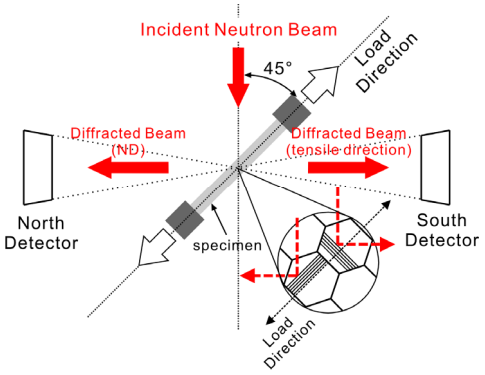

Figure 1 Schematic illustration showing an alignment of a tensile test specimen with respect to the incident and diffracted neutron beam.

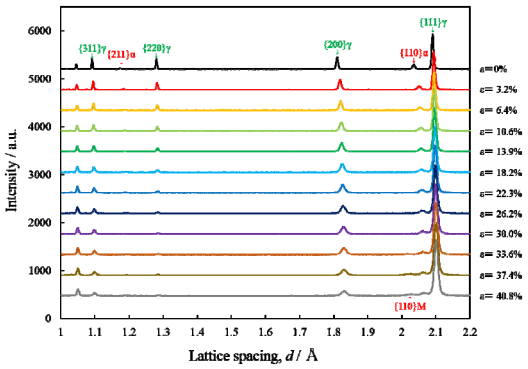

Figure 2 *In-situ* neutron diffraction profiles during tensile deformation of the 0 % cold-rolled Fe-24Ni-6Al-0.4C.

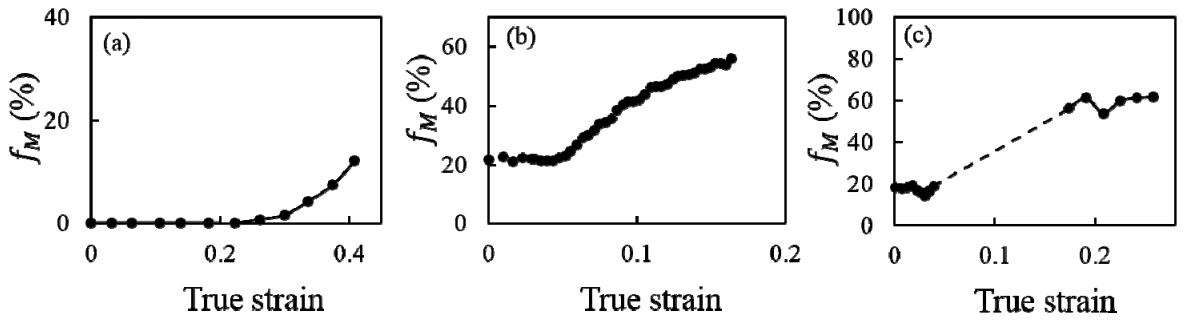

Figure 3 Changes in fraction of martensite with increasing of the tensile strain in the Fe-24Ni-6Al-0.4C; (a) 0% cold-rolled specimen, (b) 50 % cold-rolled specimen, (c) 81 % cold-rolled specimen.

(1-2)

Deformation behavior of the dual phase (DP) steel consisting of ferrite phase and martensite phase was analyzed by *in-situ* neutron diffraction during tensile deformation. As shown in the schematic illustration of Figure 1, a tensile test specimen was mounted at the standard tensile testing system at BL19 TAKUMI as that the tensile axis to be aligned 45° with respect to the incident beam.

Figure 4 shows changes in phase stresses (elastic stresses) of ferrite phase and martensite phase derived from lattice strains of (011) plane perpendicular to the tensile axis. It is found that large phase stress was partitioned in martensite phase and that the difference of phase stress between martensite phase and ferrite phase increased with increasing of the applied stress.

Other than the present neutron diffraction experiment, we have evaluated local strain distribution during tensile deformation in the DP steel by digital image correlation (DIC) analysis. Figure 5 shows changes in average plastic strains of ferrite phase and martensite phase during deformation. By combining the plastic strain distribution obtained by DIC analysis and the phase stress estimated by the present neutron diffraction experiment, we successfully reconstructed stress-strain curves of ferrite phase and martensite phase in the DP steel separately (Figure 6). There are several models for predicting macroscopic stress-strain curve of the multi-phase materials by using stress-strain curves of each constituent phases. Within our knowledge, however, our result shown in Figure 6 is the first case that the stress-strain curves of ferrite phase and martensite phase in the DP steel was obtained separately from the experimentally obtained macroscopic stress-strain curve.

(1-3)

Deformation behavior of dual phase Cu-Zn alloy during tensile deformation was also investigated by *in-situ* neutron diffraction. We confirmed that phase transformation occurred during deformation.

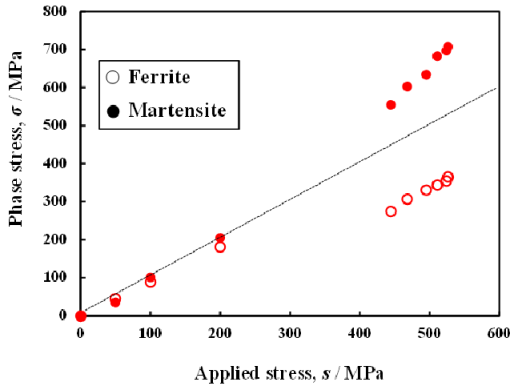

Figure 4 Changes in phase stresses (elastic stresses) of ferrite phase and martensite phase during tensile deformation in the DP steel obtained by neutron diffraction analysis.

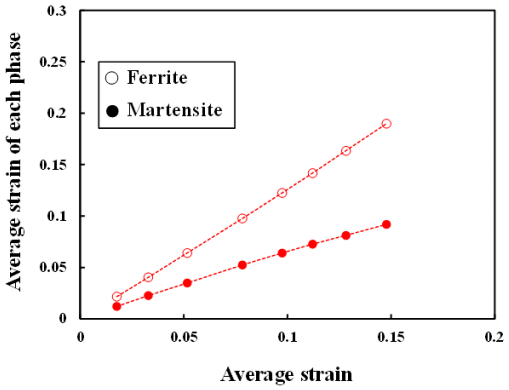

Figure 5 Changes in average plastic strains of ferrite phase and martensite phase during tensile deformation in the DP steel obtained by DIC analysis.

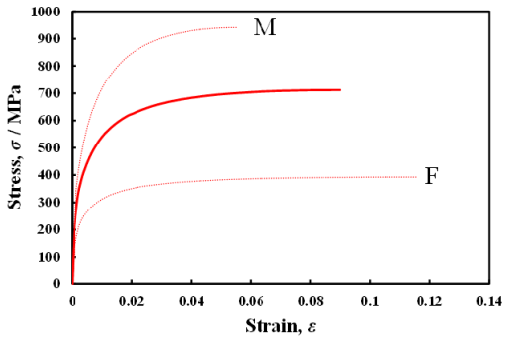

Figure 6 Stress-strain curves of ferrite phase (F) and martensite phase (M) in the DP steel reconstructed by combination of *in-situ* neutron diffraction analysis and DIC analysis.

(2) 5/16, 17, 19, 20, 2016

(2-1)

Dynamic ferrite transformation is a ferrite transformation occurring during deformation of austenite. Nowadays, thermomechanical controlling process utilizing dynamic ferrite transformation has been received much attention because an ultrafine-grained ferrite structure with grain size less than 1 μm can be achieved. So far, however, many aspects of dynamic ferrite transformation, such as deformation condition for the occurrence of dynamic ferrite transformation, formation mechanism of the ultrafine-grained structure, partitioning behavior of elements, and so on, have not been fully understood yet.

In the present experiment, we investigated elements partitioning behavior of dynamic ferrite transformation by *in-situ* neutron diffraction analysis during compression at elevated temperature using a newly developed thermomechanical processing simulator installed at BL 19 TAKUMI. Figure 7 represents an appearance of the thermomechanical processing simulator and a schematic illustration for an alignment of a specimen with respect to the incident and diffracted neutron beams. The specimen was austenitized at 1000 °C for 300 s, and cooled to the deformation temperature ranging from 650 – 750 °C. Then, uniaxial compressive deformation by at most 60 % was applied at the temperature. Strain rate for the compressive deformation was 1×10^{-3} s^{-1}. The specimen was placed between two anvils (c-BN) in the chamber, and heated by induction heating system. The chamber moves upward by the half of deformation amount so that neutron beam is always irradiated at the center of the specimen during compression experiment.

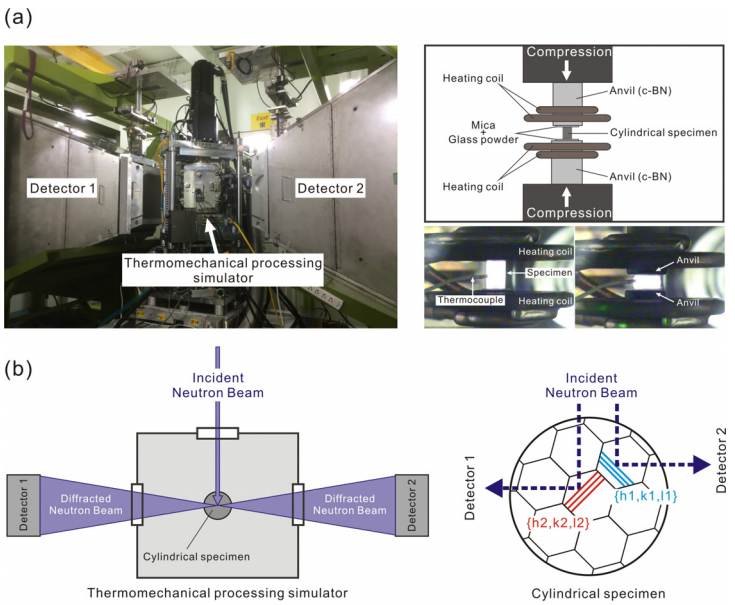

Figure 7(a) The thermomechanical processing simulator installed at the BL 19 TAKUMI, and schematic illustration of the testing part of the simulator, (b) The geometry of the compression experiment with respect to the incident and diffracted neutron beams.

Figure 8 shows changes in lattice constants of statically transformed ferrite and dynamically transformed ferrite (strain rate: 10^{-3} s^{-1}) obtained by Rietveld analysis. As shown in Figure 8, the lattice constants of statically transformed ferrite (triangles) did not change during transformation. In contrast, the

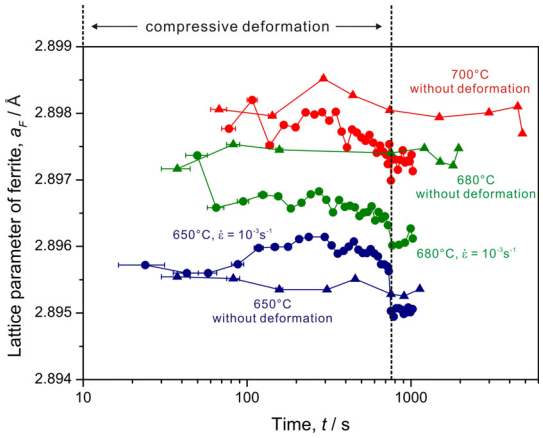

Figure 8 Change in lattice constants of statically transformed ferrite (triangles) and dynamically transformed ferrite (circles) during transformation.

lattice constants of dynamically transformed ferrite (circles) decreased during transformation. The same tendency was also confirmed in the previous experiment (2014E0003) with the strain rate of 10^{-2} s^{-1}. It should be noted that the decrease in lattice constant of dynamically transformed ferrite was opposite tendency from the elastic strain by compressive deformation. The results suggest that partitioning behavior of elements in dynamic transformation changed with proceeding the transformation, i.e., para-equilibrium partitioning to ortho-equilibrium partitioning.

(2-2)

It has been reported that medium Mn steels which contain a certain amount of retained austenite exhibits excellent mechanical properties. In order to improve mechanical properties of medium Mn steels much more through thermomechanical controlling process, it is necessary to understand the formation mechanism of retained austenite. In the present experiment, we investigated reverse transformation behavior of the medium Mn steel by using the newly developed thermomechanical controlling simulator. We are now analyzing the obtained neutron diffraction profiles.

(2-3)

Titanium and Titanium alloys are widely used in aeroplane and space applications, because of their light weight, excellent high-temperature strength and corrosion resistance. Aeroplane parts of Titanium alloys are fabricated through hot forging at elevated temperatures after melting and casting. The hot deformation (forging) is carried out in beta single-phase region as well as in alpha + beta two-phase region, so that complicated microstructures are maintained to achieve appropriate properties. However, a number of phenomena happening during such thermomechanical controlling processes are still unclear. In the present experiment, we investigated phase transformation behavior of Ti-6Al-4V alloy during deformation at elevated temperature by using the newly developed thermomechanical controlling simulator. We are now analyzing the obtained neutron diffraction profiles.